ENGINEERING RESEARCH INSTITUTE
UNIVERSITY OF MICHIGAN
ANN ARBOR

PROGRESS REPORT NO. 3

RESEARCH DESIGN PROBLEMS RELATING TO FACILITIES FOR SIMULATING THE AERODYNAMIC EFFECTS OF ATMOSPHERIC GUSTS ON AIRCRAFT COMPONENTS

April 26, 1953 - July 26, 1953

By

A. M. KUETHE

J. D. SCHETZER

L. C. GARBY

Project 2099

WRIGHT AIR DEVELOPMENT CENTER, U.S. AIR FORCE
CONTRACT AF 33(616)-316, E.O. R-465-6 BR-1

August, 1953

SUMMARY

A moving-bump device for generating the nonstationary aerodynamic effect of atmospheric gusts has been tested. Associated instrumentation has been developed that can measure the significant quantities to within 12 per cent. This estimation of the accuracy was obtained by combining uncertainties in the measurement in the least favorable fashion. The repeatability obtained and a qualitative check of measured lift lag against theoretical results indicate that the moving-bump system, if scaled up to a higher Reynolds number, is a satisfactory gust-generating device.

Installation of the vortex generator is complete and fabrication of a balance system is in process.

PROGRESS REPORT NO. 3

RESEARCH DESIGN PROBLEMS RELATING TO FACILITIES FOR SIMULATING THE AERODYNAMIC EFFECTS OF ATMOSPHERIC GUSTS ON AIRCRAFT COMPONENTS

I. MOVING BUMP

Most of the present period was used to put the bump system and its instrumentation in order and to obtain test data from which the moving bump as a gust-generating device can be appraised. The physical operation of this system has been described in the previous progress reports.

The two techniques used to determine the effectiveness of the bump as a gust generator are:

a. Comparison of dynamic and quasi-steady lift developed by an airfoil.

b. Measurement of the flow angle at the test section during the bump motion.

Both of these experimental techniques are described below.

Determining Bump Effectiveness by Means of Airfoil Lift

In this technique the effectiveness of the bump is evaluated by comparing the lift developed on an airfoil in a quasi-steady flow with that on the same airfoil in a true nonstationary flow.

Figure 1a is a photograph of the airfoil mounted in the tunnel. Figure 1b is a close-up of the airfoil-balance configuration. Only the center span is sensitive to lift; the two end sections serve only to reduce tip effects. The wing has an NACA 0018 airfoil contour with a 6-inch chord and a span of 12 inches. In order to keep the mass of the airfoil small, the contour has been carved from foam polystyrene plastic and its surface covered with model-airplane tissue paper. To provide additional rigidity and attachment points at the ends of the span, an aluminum tube of 3/4-inch diameter and

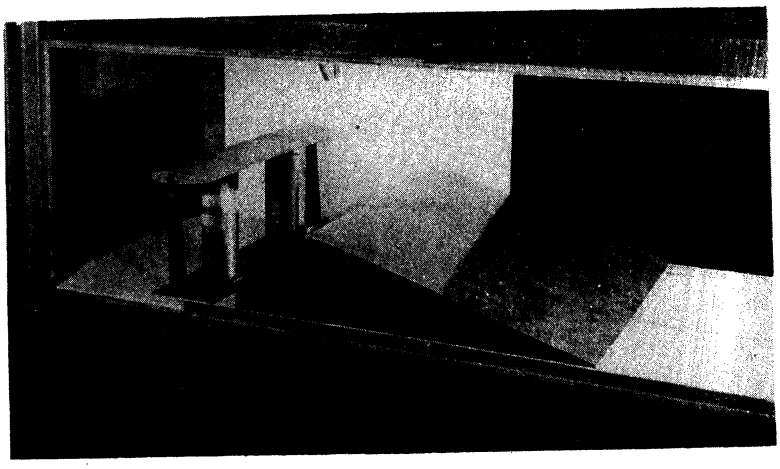

Fig. 1a. View of Airfoil Mounted in the Test Section.

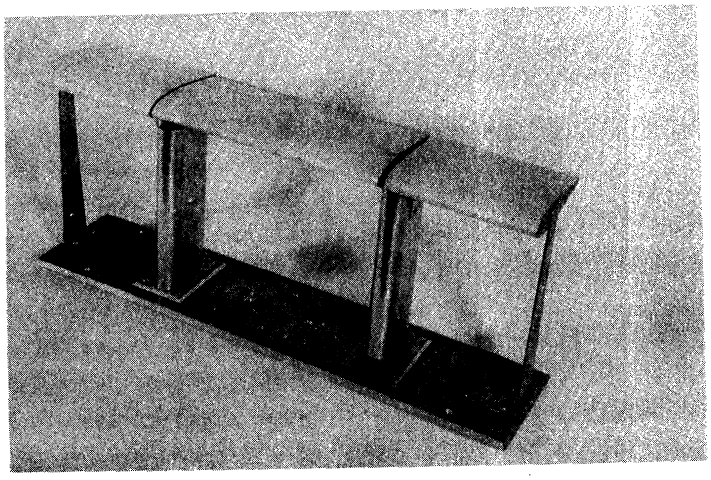

Fig. 1b. View of Lift Sensitative Airfoil.

1/32-inch wall thickness was placed through the center of the airfoil. To each end of this tube was attached a 1/16-inch-thick aluminum plate having the shape of the airfoil. A sketch of the wing construction is shown in Fig. 2.

The balance system used is shown in Fig. 3. One end of the airfoil's span is hinged so that it can rotate only about the chord axis. The hinge was made with tolerances sufficiently close to prevent motion due either to pitching moment or to drag. The motion of the wing due to lift is restrained at the other end of the span by means of a cantilever beam. An extension of this beam is used to actuate a Schaevitz transformer core and provides a 10:1 displacement magnification relative to the wing motion. An oil damping system is necessary to reduce oscillations picked from vibrations of various components.

The Schaevitz linear deflection transformer is fed with a 20,000-cps signal. The output from the transformer is amplified and then demodulated. The entire electrical system consisting of an oscillator, amplifier, and demodulator is contained in a single chassis. The unit's trade name is "Dynamike". The output from the "Dynamike" is fed directly to the y axis of the scope. A filter circuit was installed to eliminate a 100-cps noise which was present in the system. This filter has no noticeable effect upon the 5-10-cps wave which is the basic component of the dynamic trace.

In order to reduce turbulence and other fluctuations, the tunnel was changed from a closed-circuit to an open-circuit channel and 5 screens were inserted in the setting chamber. Even with the flow-circuit changes made, some large flucuations of a rather long period still exist. The fluctuations are random but appear to have a period of the order of 1 second. They could be due to an intermittent separation and reattachment in some portion of the tunnel circuit or to the generation of large eddies in the area surrounding the settling-chamber entrance. The technique for appraising the uncertainties that these fluctuations introduce in the measurement is described below.

Quasi-Steady Flow. The tunnel speed was set at a given value and the bump fixed at a specific point. A time-exposure photograph of 30 seconds was taken of the lift trace on the oscilloscope face. A typical oscillogram is shown in Fig. 4a. The smear is a result of the fluctuations noted above. The center of the smear is taken as the lift and the smear width is interpreted as the uncertainty. This process is repeated at a series of bump positions.

Dynamic Tests. In this case, for each run, only one sweep across the oscilloscope is made, and a photograph of it is obtained. A typical oscillogram is shown in Fig. 4b. Uncertainties due to tunnel fluctuations are appraised by repeating a number of runs. To make the comparison between runs,

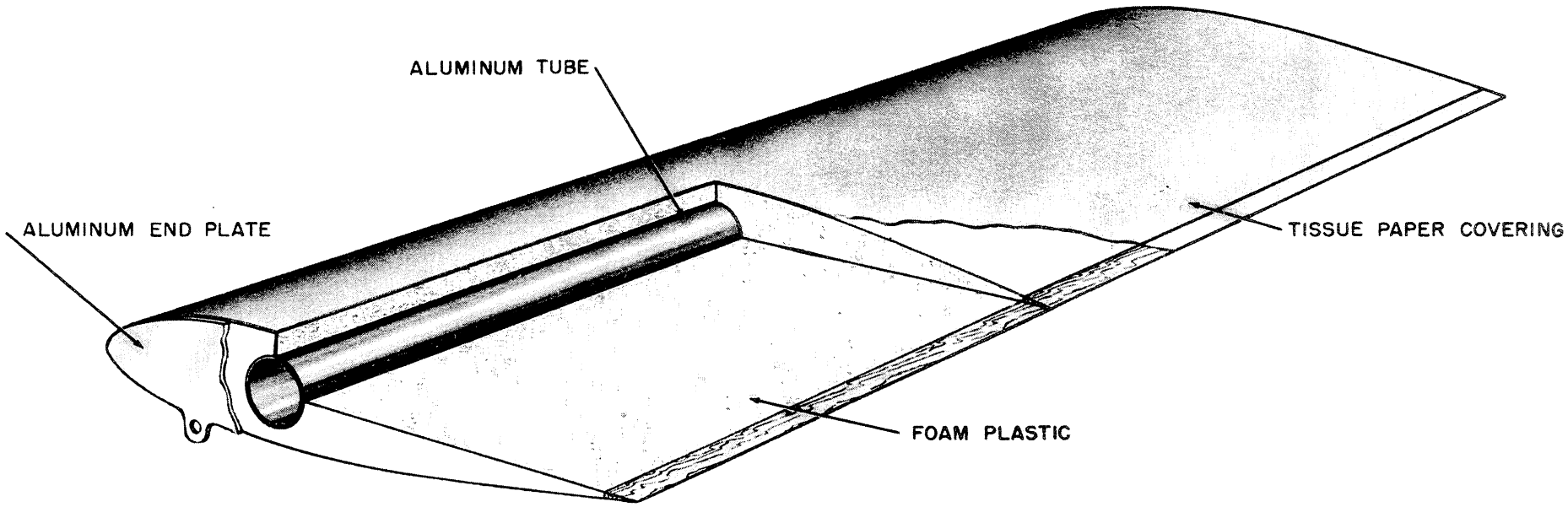

FIG. 2

CUT-AWAY OF BALANCE AIRFOIL

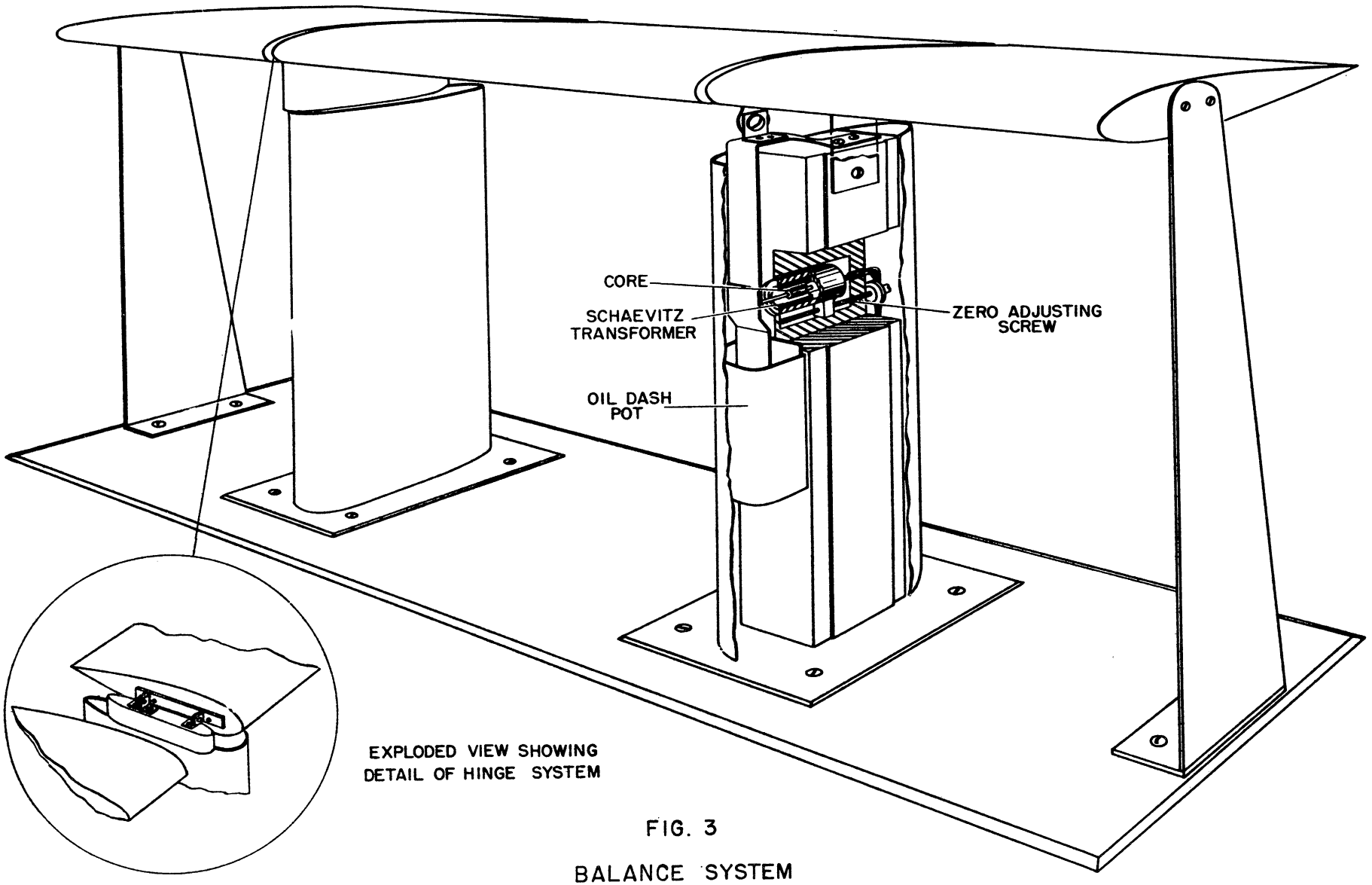

FIG. 3

BALANCE SYSTEM

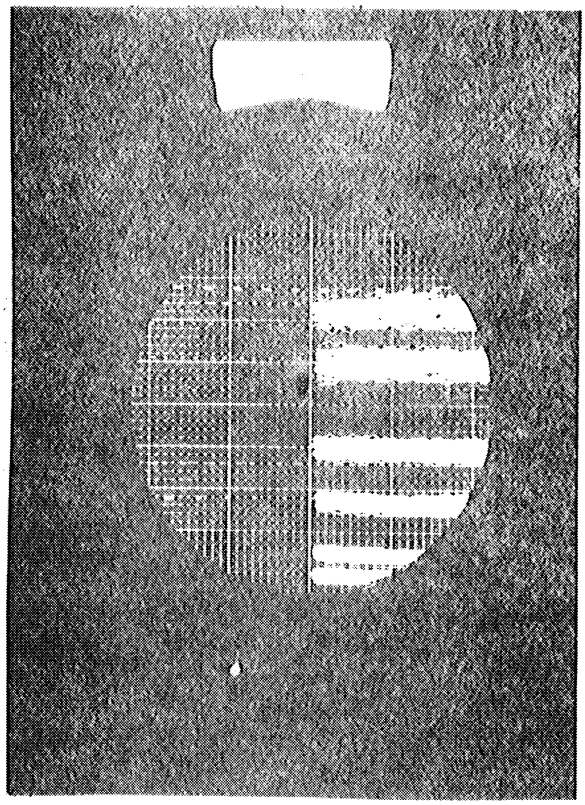

Fig. 4a. Oscillogram of Quasi-Steady Lift.

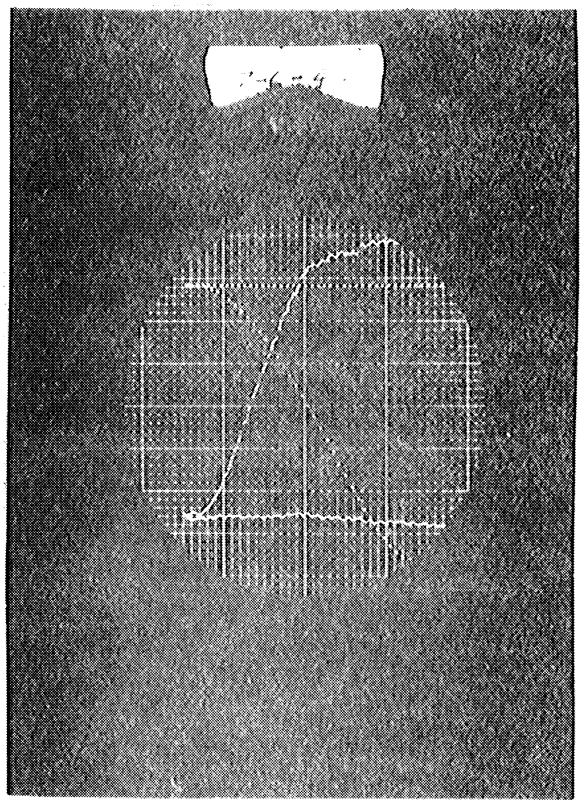

Fig. 4b. Oscillogram of Dynamic Lift Case. Solid Trace is the Lift Response. Dotted Trace is the Bump Position, Period between Dots is 1/50 sec.

the initial lift of the airfoil is recorded before the bump starts moving and this is used as the reference level for that particular run.

Calibration of Lift. The calibration of the lift force was accomplished by using a pan balance and loading the airfoil in the positive-lift direction. The response of the balance system appeared to be good and there was no observable scatter in data. A photograph of the lift-load-calibrating mechanism is shown in Fig. 5.

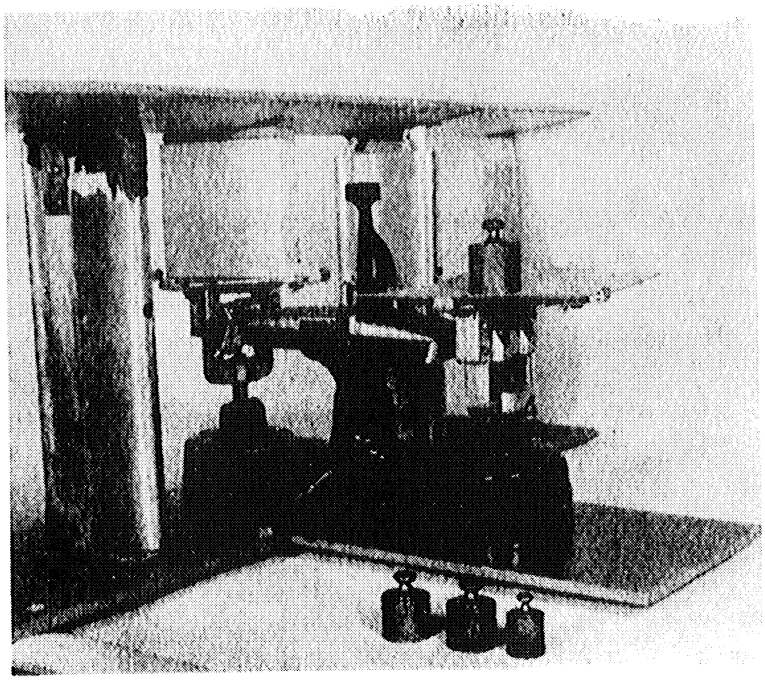

Fig. 5. View of Balance Calibrating System.

Measurement of Flow Angles

The effect of the bump in producing a change in flow direction was observed in two ways: by means of a hot-wire anemometer using an X wire configuration, and by means of a yaw-sensitive cylinder. With the hot-wire anemometer both the quasi-steady- and dynamic-flow angles were measured. In the case of the yaw-sensitive cylinder only the quasi-steady-flow angles could be measured. Both of these techniques are described below.

Hot Wire Measurements. The hot wire was used to measure the flow angle for both quasi-steady and dynamic conditions. Angle calibrations of the hot wire were obtained by setting the bump at a series of fixed stations and rotating the X probe head through a series of angles. Thus a separate calibration curve was obtained for each bump station. As in the case of the airfoil-lift technique, fluctuation of the flow level in the tunnel occurred, and a method similar to that described above was used to appraise the resulting uncertainty.

Flow Angles by Means of Pressure Measurements: In order to provide an independent check on the flow directions as obtained by the X hot-wire probe for the quasi-steady case, a yaw-sensitive pressure probe was used. The probe consisted of a cylindrical tube of 0.12-inch diameter with three pressure orifices spaced on the perimeter at 60° intervals. The flow angle was determined by adjusting the probe angle until the pressure response from the two outer orifices was exactly equal. A Betz-type water micromanometer was used to determine the null point.

Geometry of Measurement

The reference system and location of the test equipment is as follows:

A rectangular coordinate system is used to locate points within the test section. The origin of the coordinate system is located on the floor of the tunnel, midway between the two side walls, and 2-1/4 inches downstream from the test-section entrance. The scale unit along all axes is in inches. The coordinate axes are denoted as follows:

x axis - extends along the flow direction; positive sense is downstream.

y axis - lies in the horizontal plane and is normal to the wind direction; positive sense follows from the right-hand rule.

z axis - extends in the vertical direction; positive sense is upward.

Tabulated below are the locations of the test units within the test section.

Item	Location in Inches		
	x	y	z
Test-Section Dimensions	-2.25 +102.0	±14.9	+21.1
Bump; Leading-Edge Position			
Forward	+19.2		
Retracted	+63.0		
Airfoil			
Leading Edge	+9.5		+10.5
Trailing Edge	+15.5		+10.5
Hot-Wire Probe	+16.8	0	+10.5
Angle of Attack of Pressure Probe	+16.5	+3.9	+10.5

Data Obtained

The technique used in obtaining the data is described in the previous section. In this section, the experimental results are shown and discussed for the moving-bump system.

Figure 6 shows the quasi-steady lift force as a function of bump position for a constant tunnel speed. Five runs were taken under similar conditions. A curve has been drawn through the arithmetic mean of the test data and the scatter is interpreted as an uncertainty.

Figures 7 through 10 show the dynamic tests. Each of these figures represents a series of runs at a particular shock-cord tension. The range of bump speeds for each run is indicated on the figure. All tests were conducted at constant tunnel speed of 34 feet per second. The lift of the airfoil and bump position are plotted versus time in these curves. The plot of bump position versus time has been compensated to take into account a shift in the zero reference.

Figure 11 shows a cross plot of lift versus bump position of the dynamic runs taken from the curves of Figs. 7 through 10. The quasi-steady plot of lift versus bump position is taken from Fig. 6.

The difference between the quasi-steady and dynamic responses is represented in Fig. 12 as lift lag versus bump position. In Fig. 13 the lift lag versus time is presented. In this figure only data from the first and fourth tests are plotted, since they represent in general the upper and lower limits of the lift lag.

A comparison of the results of Fig. 13 with theory and a discussion of errors is given below.

Figure 14 shows the measured values of flow deflection as a function of bump position for quasi-steady and dynamic flow using hot wire, and quasi-steady flow measured by means of the pressure probe. As expected, the quasi-steady and dynamic results agree when adjustments for zero shift are made.

Discussion of Errors and Comparison with Theory

Figures 12 and 13, which represent the lift lag versus bump position and time respectively, have uncertainties in both ordinate and abscissa. These may be described as follows. The measured lift at any bump position in the quasi-steady test (Fig. 6) is uncertain because of electrical and flow fluctuations. The plot represents the arithmetic mean of several runs, and

FIG. 6

AIRFOIL LIFT VS BUMP POSITION FOR QUASI-STEADY FLOW

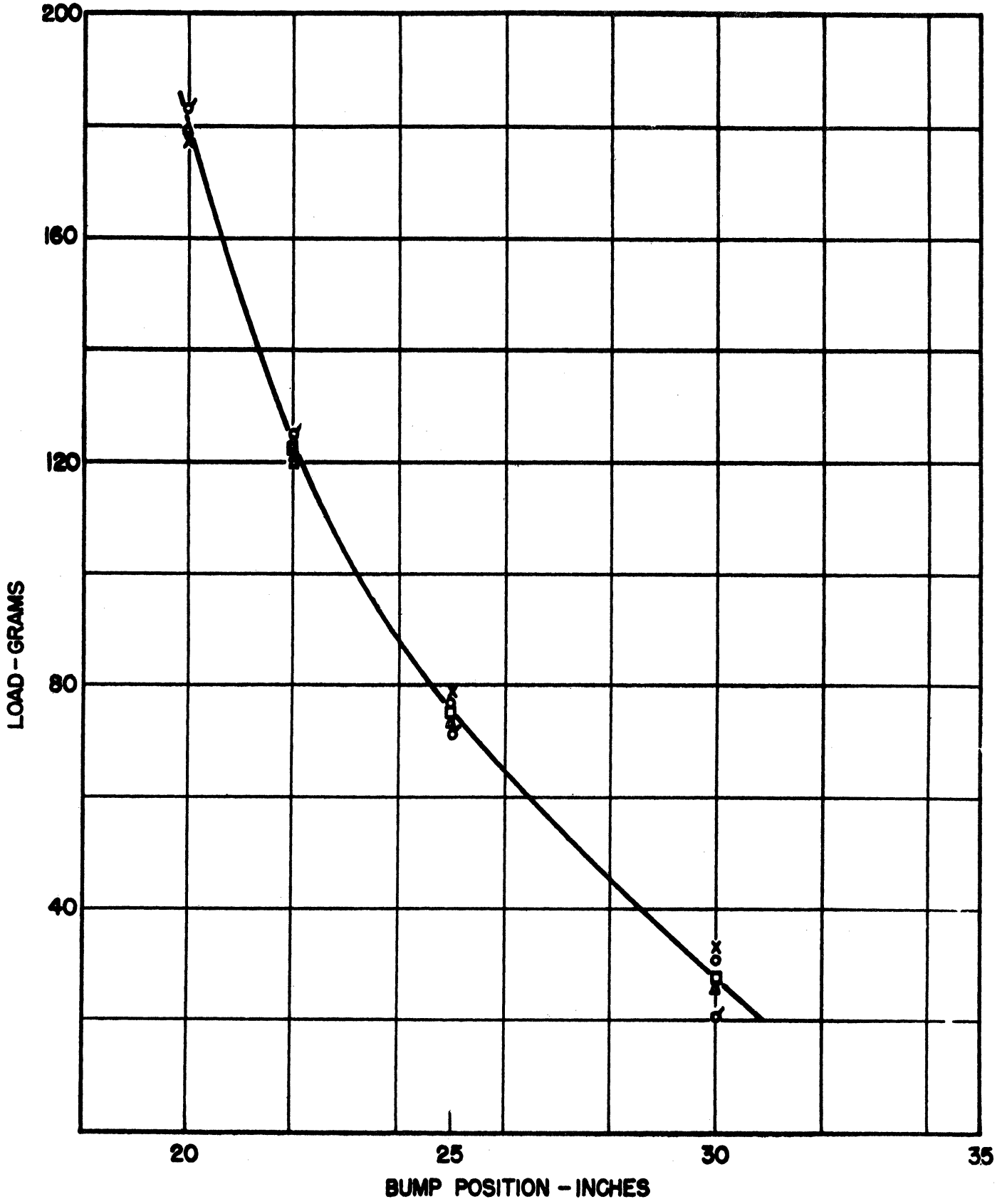

FIG. 7

AIRFOIL LIFT AND BUMP POSITION VS TIME FOR DYNAMIC TEST NO. 1

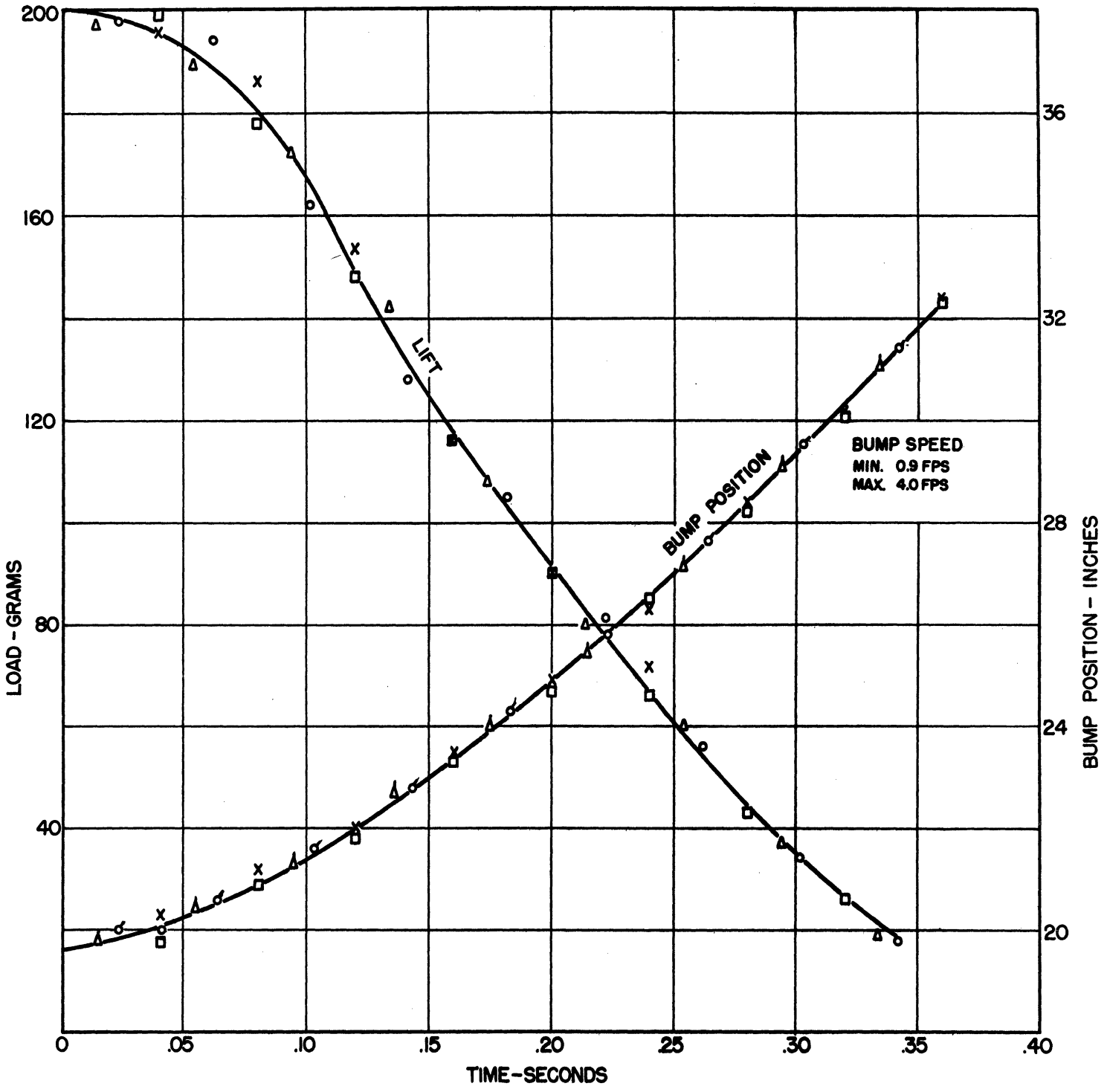

FIG. 8

AIRFOIL LIFT AND BUMP POSITION VS TIME FOR DYNAMIC TEST NO. 2

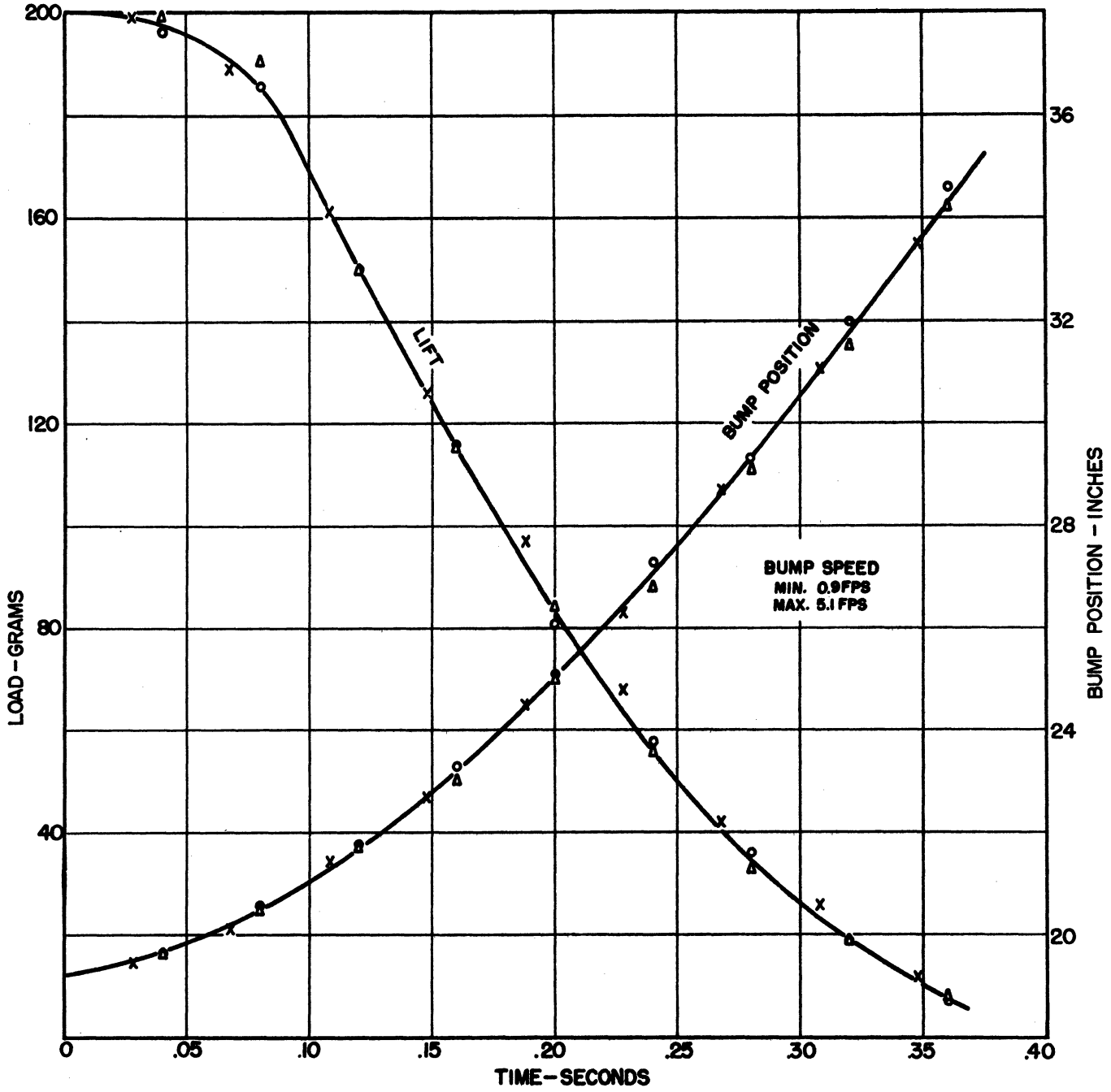

FIG. 9

AIRFOIL LIFT AND BUMP POSITION VS TIME FOR DYNAMIC TEST NO. 3

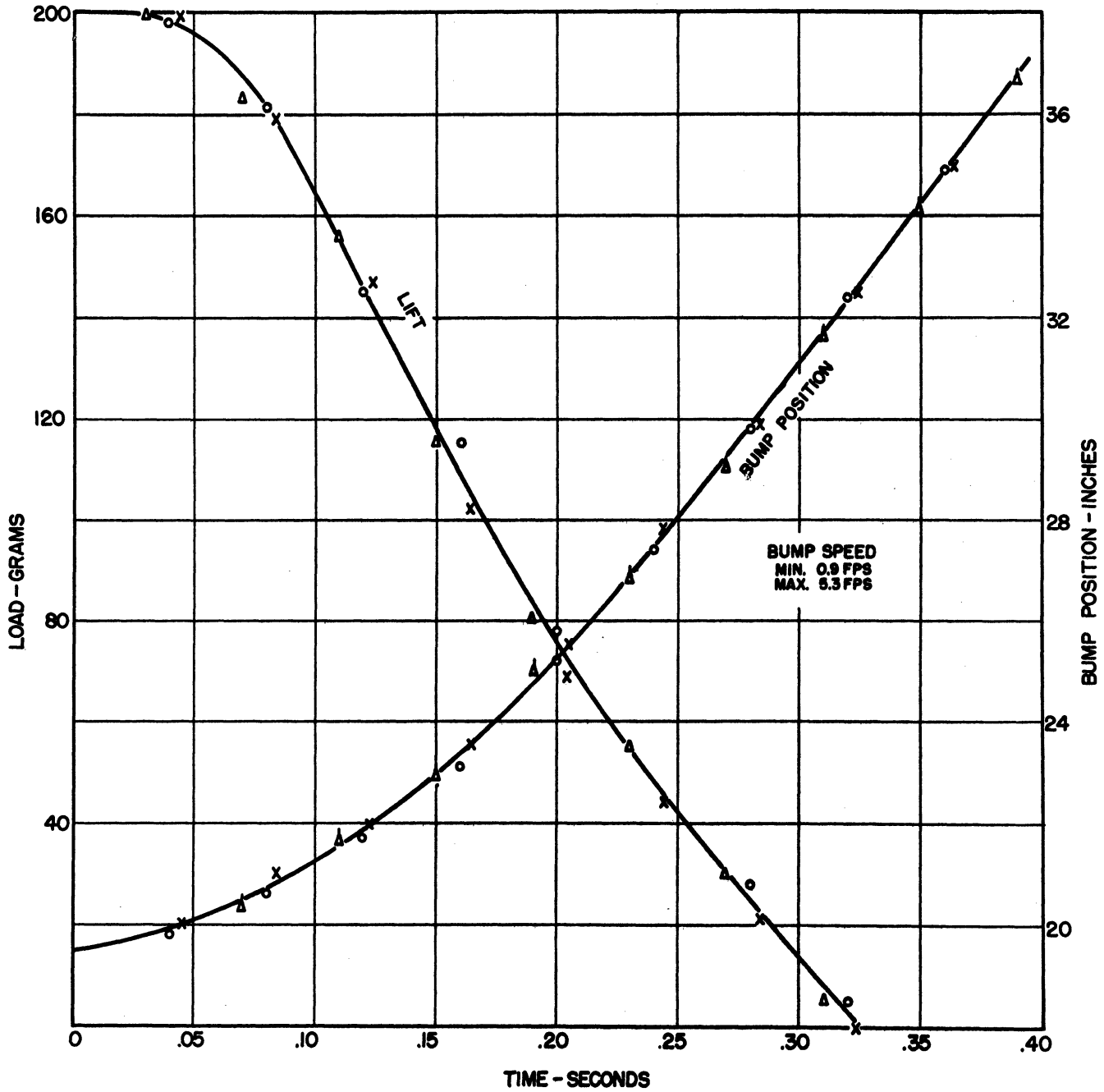

FIG. 10

AIRFOIL LIFT AND BUMP POSITION VS TIME FOR DYNAMIC TEST NO. 4

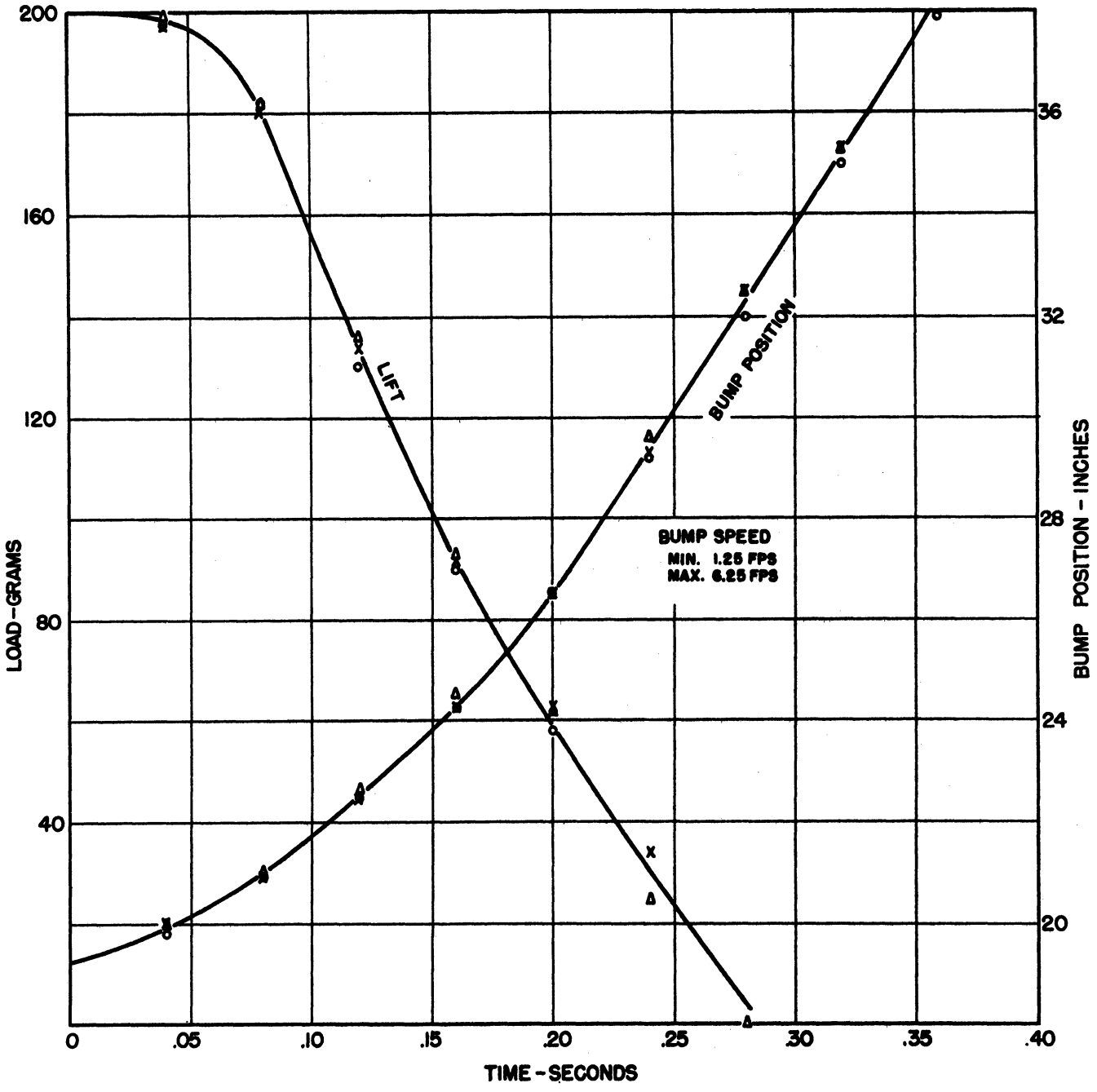

FIG. 11

COMPARISON OF AIRFOIL LIFT VS BUMP POSITION FOR THE DYNAMIC TESTS AND QUASI-STEADY TEST

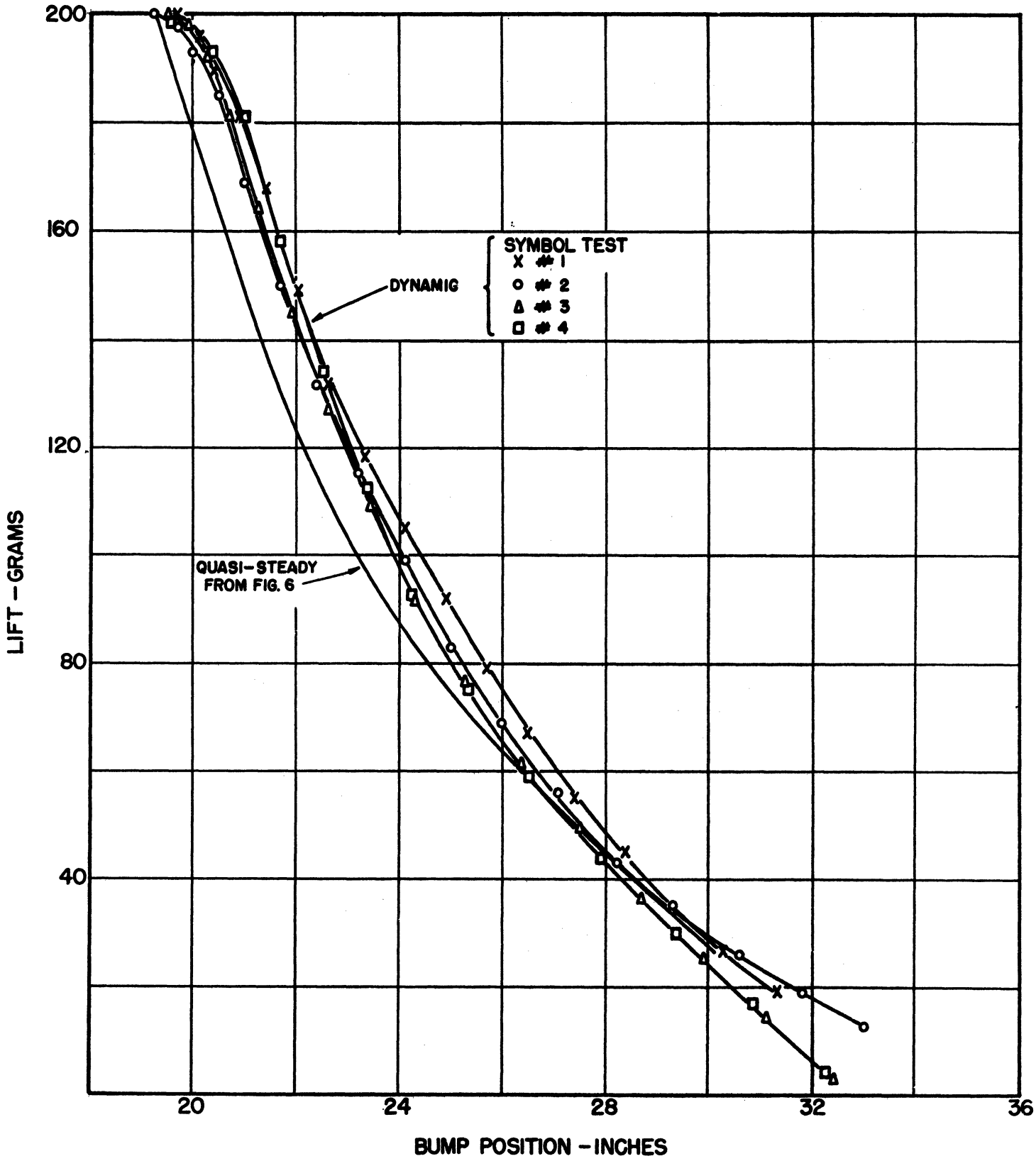

FIG. 12

AIRFOIL LIFT LAG VS BUMP POSITION

WHERE: LIFT LAG = [DYNAMIC LIFT - QUASI-STEADY LIFT] AT THE SAME BUMP POSITION

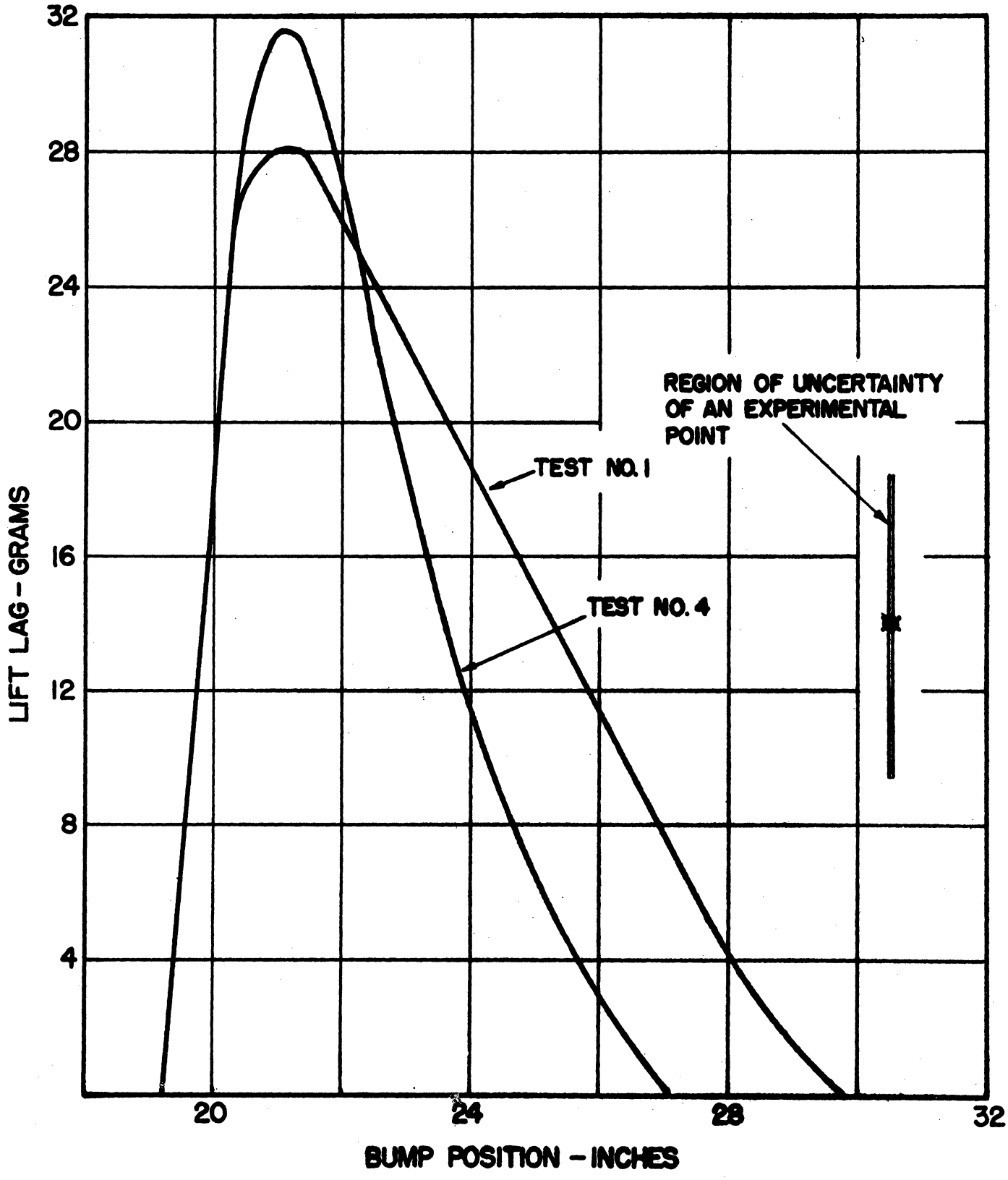

FIG. 13

AIRFOIL LIFT-LAG VS TIME

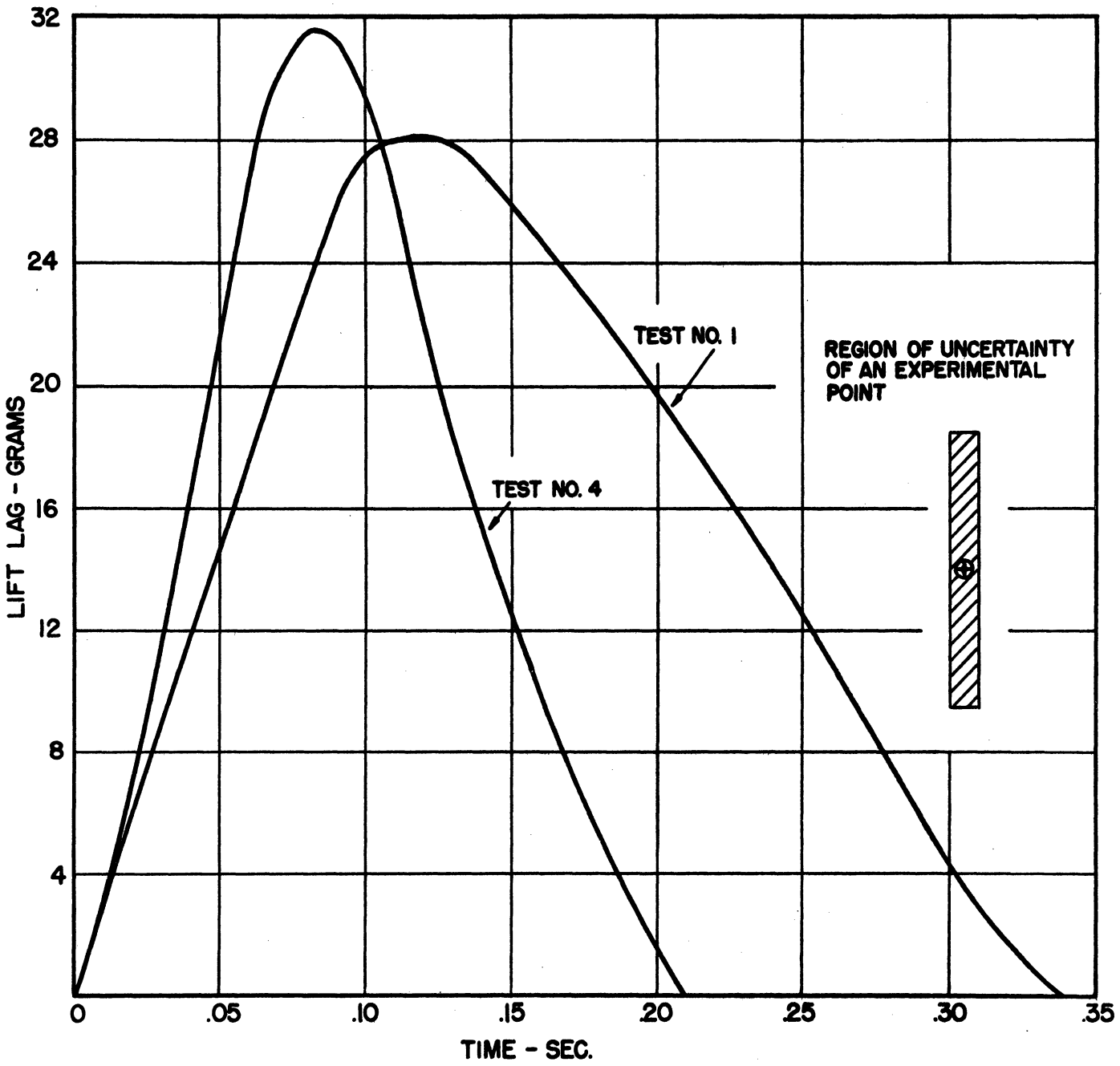

ZERO REF. ON TIME SCALE CORRESPONDS TO START OF BUMP MOTION

FIG. 14

ANGLE OF FLOW DEFLECTION VS BUMP POSITION AT TRAILING EDGE POSITION OF AIRFOIL

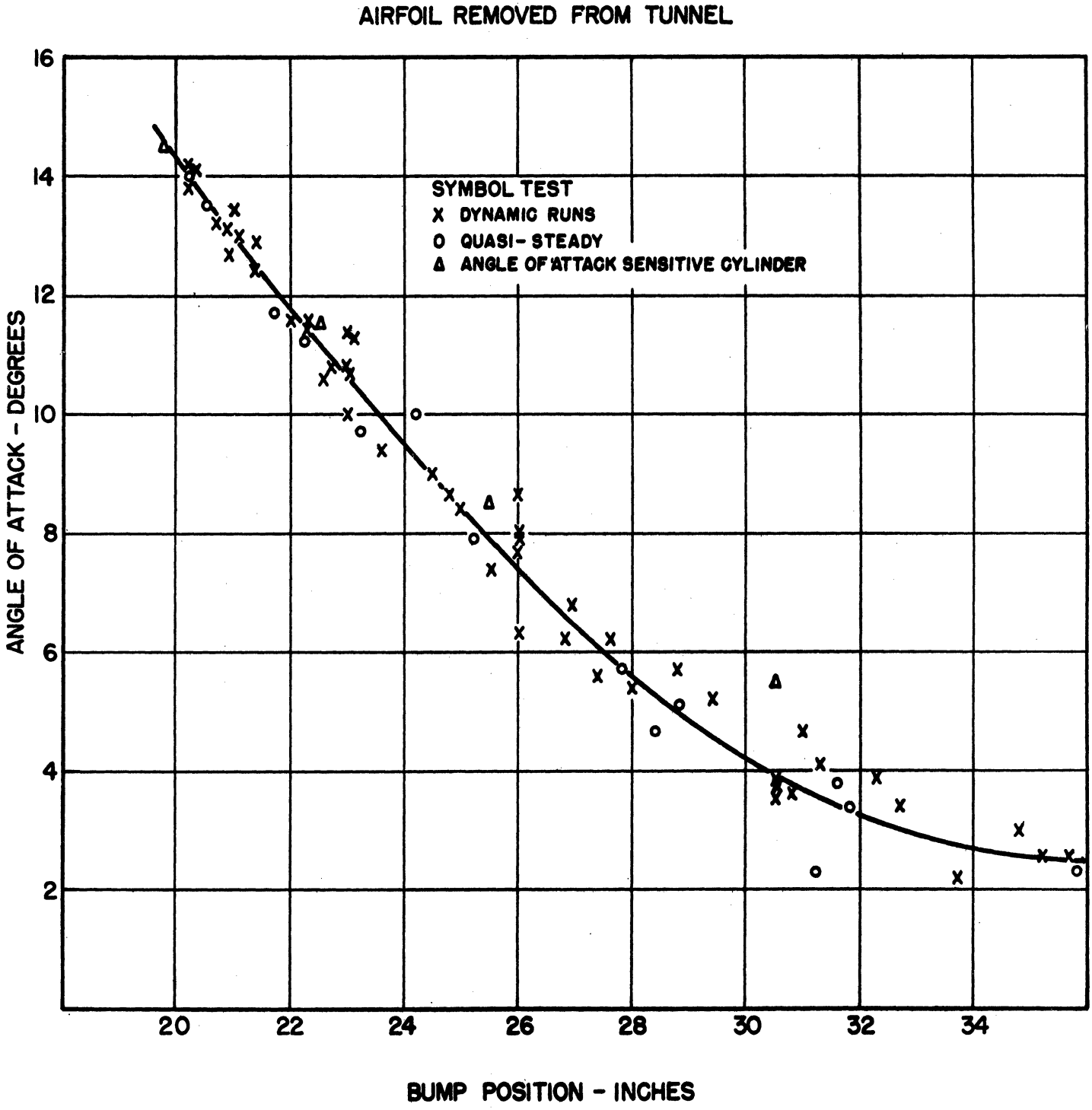

the average deviation from the mean curve is ±2.4 grams in lift at any bump position. In the dynamic runs (Figs. 7 through 10) time is the independent variable and measured values of bump position and lift are plotted as ordinates. The average uncertainties in these curves are recorded below.

Test	Average Uncertainty	
	Bump Position inches	Lift Force, grams
Quasi-Steady	0	±2.4
Dyn. No. 1	±0.09	±2.2
Dyn. No. 2	±0.11	±1.2
Dyn. No. 3	±0.09	±2.0
Dyn. No. 4	±0.12	±1.9

Therefore, the uncertainties in the dynamic runs versus bump position plotted in Fig. 11 must be expressed by two numbers in order to indicate the uncertainties in both axes. These data are given in the table above. The quasi-steady lift shown on the same figure has an uncertainty in lift only of ±2.4 grams as stated above.

Therefore, the final result as represented by Figs. 12 and 13 have uncertainties in both axes of the following magnitudes:

	Run 1	Run 4
Lift Lag	±4.6 grams	±4.3 grams
Bump Position	±0.09 inch	±0.12 inch
Time	±0.01 second	±0.01 second

These uncertainties are indicated by rectangles on the figures. The average uncertainty in the measurement of lift lag is approximately 12 per cent of the maximum lift lag.

In Fig. 14 the angle of flow deflection at the position of the airfoil trailing edge (with airfoil absent) is plotted for the range of bump positions. Test data was taken for both quasi-steady and dynamic conditions. The curves have been adjusted to agree at the forward bump position in order to eliminate zero shift errors. The quasi-steady and dynamic data are in agreement, as expected. The average uncertainty in angle of attack is ±0.35° from the faired curve of Fig. 14.

Theoretical calculations for the flow pattern measured in the tunnel have not been made. However, the theory used to design the tunnel is based on a flow that is qualitatively similar to the one measured and therefore a comparison with these calculations is of qualitative interest. The design calculations are based on a constant ratio of bump speed V_b to tunnel speed V_∞ of 0.14 and a linear decrease of local angle of attack v/V_∞ from 11° to 0° in two airfoil chord lengths. The maximum lift lag from these calculations is 40 grams. The measured value of the maximum lift lag is 32 grams.

The measured value of V_b/V_∞ varies during the run from a minimum of 0.12 to a maximum of 0.19 as may be seen in Figs. 7 through 10. Furthermore, the measured v/V_∞ does not decrease linearly from 11° to 0° in two chord lengths. Figure 14 shows that it tends to decrease more steeply at the beginning of the run. The comparative theoretical and experimental lift lags therefore have no quantitative significance. The comparison does indicate, however, that the measured lift lag is of the right order of magnitude.

The present tests were conducted at a Reynolds number of 110,000, which is considered to be too low to duplicate accurately free-flight, nonstationary phenomena.

Appraisal of Bump System

The degree of repeatability obtained in the flow-pattern measurement indicates that the bump system is a practical method of generating nonstationary flow. The lift-lag results indicate that refined instrumentation can be developed which will adequately measure the nonstationary results. It appears that if the present device is scaled upward to a Reynolds number greater than 500,000 it will be an adequate method of generating gusts.

II. VORTEX GENERATOR

The installation of the vortex generator was completed in this period. The design of the balance system is completed and fabrication is in process. The remaining instrumentation is the same as that used for the bump system.

III. WORK PLANNED FOR NEXT PERIOD

In the next period it is expected that the following will be accomplished:

1. The vortex generator will be placed in operation and data obtained.

2. Development of instrumentation will be continued.

3. A conference with Air Force representatives will be requested for the purpose of obtaining authorization to proceed with design and construction of gust generation on a larger scale. The purpose of the larger scale is to obtain gust-simulative tests at Reynolds numbers permitting extrapolation to flight conditions.